Iran J Orthod. 2026 December; 21(2):e1502. doi:10.32592/ijorth.21.2.1502.
Published online 2026 December 1 Research Article
Original Article **Open Access**

Comparison of the Physicochemical, Mechanical, Surface, and Antimicrobial Properties of Orthodontic Acrylic Resin with Chemically Synthesized and *Rheum palmatum*-mediated Silver Nanoparticles

Ali Ghaboos [1], Farzaneh Golfeshan [2*], Mohammad Motamedifar [3]

[1] Resident, Department of Orthodontics, School of Dentistry, Shiraz University of Medical Sciences, Shiraz, Iran
[2] Assistant Professor, Department of Orthodontics, School of Dentistry, Shiraz University of Medical Sciences, Shiraz, Iran
[3] Professor of Medical Microbiology HIV/AIDS Research Center, Research Institute for Health. Shiraz University of Medical Sciences, Shiraz, Iran

***Corresponding author:** Farzaneh Golfeshan

Address: Department of Orthodontics, School of Dentistry, Shiraz University of Medical Sciences, Shiraz, Iran.

Email: golfeshanfa@gmail.com

Received: 2026 October 17; **Revised:** 2026 November 04; **Accepted:** 2026 November 16

Abstract

Aim: Silver nanoparticles (AgNPs) may modify orthodontic acrylic resins, and the synthesis route may influence their performance. This study compared several characteristics of chemically synthesized trisodium citrate-stabilized AgNPs (AgNP-TSC) and *Rheum palmatum*-mediated AgNPs (AgNP-root).
Methods: AgNPs were incorporated into acrylic resin at 0.05% and 0.2% (w/w). Particle size and morphology were assessed by dynamic light scattering (DLS) and transmission electron microscopy (TEM). Flexural properties were measured by a three-point bending test and surface roughness by atomic force microscopy. Antimicrobial activity against Lactobacillus acidophilus, *Streptococcus mutans*, and *Candida albicans* was evaluated using an eluted component test (ECT) and a biofilm assay. ANOVA or Kruskal–Wallis tests were used with appropriate post hoc comparisons.
Results: TEM showed a smaller mean particle size for AgNP-TSC than AgNP-root (16.5 vs. 32.3 nm), but broader distribution and greater apparent aggregation. DLS intensity-weighted mean diameters were 158.15 and 223.80 nm, respectively. Neither formulation significantly affected flexural strength or surface roughness, but flexural modulus decreased significantly only with 0.2% AgNP-TSC ($P<0.0001$). In the ECT assay, both AgNP-root concentrations significantly reduced *L. acidophilus* counts, while 0.2% AgNP-root reduced *S. mutans* counts compared with the control. For *C. albicans*, a significant difference was observed only between the 0.05% AgNP-root and 0.05% AgNP-TSC groups. Biofilm outcomes did not differ significantly across the five groups.
Conclusion: AgNP-root showed a narrower TEM size distribution, lower apparent aggregation, and antimicrobial effects without significant changes in the mechanical or surface properties of the acrylic resin nanocomposites. Further research should establish long-term performance, safety, and clinical relevance.

Keywords: Antimicrobial activity, Flexural properties, Orthodontic acrylic resin, *Rheum palmatum*, Silver nanoparticles.

Copyright © 2026, Author(s). This is an open-access article distributed under the terms of the Creative Commons Attribution-NonCommercial 4.0 International License (http://creativecommons.org/licenses/by-nc/4.0/) which permits copy and redistribute the material just in noncommercial usages, provided the original work is properly cited.

Background

Removable orthodontic appliances are widely used for retention following fixed orthodontic treatment and for selected functional and tooth-movement therapies. However, their acrylic resin components can promote microbial adhesion and biofilm accumulation with cariogenic and opportunistic microorganisms, including Lactobacillus acidophilus (*L. acidophilus*), Streptococcus mutans (*S. mutans*), and Candida albicans (*C. albicans*), particularly when surface irregularities and inadequate oral hygiene are present (1–3). Removable orthodontic appliances are commonly fabricated from self-curing acrylic resins, with polymethyl methacrylate (PMMA) as the primary constituent (4,5). Cold-cured acrylic resins may be particularly susceptible to microbial accumulation because of their relatively lower degree of polymerization and greater porosity. Although mechanical and chemical cleaning can reduce microbial contamination, the effectiveness depends partly on patient compliance, and some chemical agents may adversely affect acrylic materials. These limitations have increased interest in resin-based materials with intrinsic antimicrobial properties (4,6,7).

Nanotechnology offers opportunities to modify dental materials by incorporating nanoparticles with distinctive physicochemical properties (8, 9). Among these materials, silver nanoparticles (AgNPs) have attracted considerable attention because of their broad-spectrum antimicrobial activity and potential applications in dental and orthodontic materials (10,11). Their high surface area facilitates interactions with microbial cells, and antimicrobial effects are attributed to silver ion release, membrane disruption, interaction with cellular proteins, inhibition of respiratory processes, and generation of reactive oxygen species (12,13). AgNP incorporation may also affect the mechanical and surface properties of acrylic polymers, depending on nanoparticle concentration, characteristics, incorporation method, and resin formulation. Increasing AgNP concentration may enhance antimicrobial activity while adversely affecting mechanical performance, highlighting the need to balance antimicrobial efficacy with preservation of clinically relevant material properties (4,6,7,10,14).

The synthesis route may further influence the physicochemical and biological characteristics of AgNPs. Conventional synthesis approaches may involve substantial energy requirements or chemical reducing and stabilizing agents. In contrast, plant-mediated green synthesis uses phytochemicals as reducing and stabilizing agents and has emerged as a potentially simpler and more sustainable alternative (15–17). The diverse secondary metabolites present in plant extracts may participate in nanoparticle formation and stabilization, potentially reducing reliance on conventional chemical reagents (18–20). Among medicinal plants investigated for nanoparticle synthesis, *Rheum palmatum* root extract is of particular interest because of its biologically active phytochemicals and reported antibacterial activity against clinically relevant bacterial species (21).

Despite increasing research on AgNP-modified dental materials and plant-mediated nanoparticle synthesis, direct comparisons of conventionally synthesized and R. palmatum-mediated AgNPs incorporated into the same orthodontic acrylic resin remain limited. Moreover, the effects of nanoparticle incorporation on acrylic resin properties may vary according to nanoparticle type, concentration, synthesis route, and experimental conditions (4,6,7,10,21). A recent meta-analysis of in vitro studies found no overall statistically significant deterioration in several physicomechanical properties after nanoparticle incorporation; however, substantial heterogeneity among studies highlights the need for standardized, direct comparisons (14). Therefore, the relationship between AgNP synthesis route, antimicrobial activity, and preservation of mechanical and surface properties remains insufficiently characterized under standardized conditions. Accordingly, this study aimed to compare the physicochemical characteristics, mechanical, surface, and antimicrobial properties of orthodontic acrylic resin nanocomposites containing different concentrations of chemically synthesized trisodium citrate-stabilized silver nanoparticles (AgNP-TSC) and green-synthesized R. palmatum-mediated silver nanoparticles (AgNP-root).

Methods

Ethical Considerations

The protocol for this in vitro study was approved by the Ethics Committee of Shiraz University of Medical Sciences, Shiraz, Iran (Approval ID: IR.SUMS.DENTAL.REC.1402.068).

Synthesis of Silver Nanoparticles

Silver nanoparticles were synthesized by chemical reduction of silver nitrate using trisodium citrate under ultrasonic irradiation. Briefly, 50 mL of 0.05 M trisodium citrate dihydrate ($Na_3C_6H_5O_7 \cdot 2H_2O$; Merck, Germany) was

transferred to an Erlenmeyer flask and placed in a sonication bath. Subsequently, 50 mL of 0.05 M silver nitrate solution ($AgNO_3$; Merck, Germany) was added dropwise to the flask over 1 h under sonication at room temperature. The mixture was then bath-sonicated for 12 h, yielding a gray suspension. The suspension was centrifuged at 8000 rpm to separate the nanoparticles from the aqueous phase. The resulting precipitate was washed five times with double-distilled water (Zalal Teb Shimi, Iran) to remove water-soluble impurities and subsequently dried in an oven at 50°C (22). The resulting dried silver nanoparticle powder was designated AgNP-TSC.

Preparation of R. palmatum Root Extract

To prepare the root extract, R. palmatum roots (LonierHerb, China) were ground using a mortar. Ten grams of the powdered material were placed in a cellulose thimble (CHMLAB, Spain) and transferred to a Soxhlet apparatus containing 200 mL of boiling double-distilled water. After 24 h of extraction, a brown suspension was obtained. The suspension was centrifuged at 10,000 rpm, and the resulting brown solution was collected and used as the reducing agent for silver nanoparticle synthesis. The solid content of the aqueous extract was determined gravimetrically. A known amount of the extract was weighed, transferred to a pre-weighed container, and dried in an oven at 60°C. The dried sample was then reweighed, and the percentage of solid content was calculated from the difference between the initial and final weights. The solid content of the prepared extract was 2.29%.

Green Synthesis of Silver Nanoparticles Using R. palmatum Root Extract

Silver nanoparticles were synthesized using R. palmatum root extract as the reducing agent. Briefly, 1.68 g of the prepared extract was diluted with double-distilled water to a final volume of 50 mL and placed in a sonication bath. Subsequently, 50 mL of 0.05 M silver nitrate solution ($AgNO_3$; Merck, Germany) was added dropwise over 1 h under sonication. After 12 h of reaction, a brown suspension was obtained. The suspension was centrifuged at 10,000 rpm and washed with double-distilled water. The resulting brown precipitate was dried at 50°C for 24 h (21). The obtained nanoparticle powder was designated AgNP-root.

Preparation of Resin Nanocomposites

To produce a self-cured orthodontic acrylic resin, the synthesized and dried AgNP-TSC and AgNP-root powders were first crushed in a mortar to obtain a suitable powder. The nanoparticles were then incorporated into the liquid component to achieve final concentrations of 0.05% and 0.2% (w/w) in the polymerized acrylic resin (Acropars, Iran). The nanoparticle-containing liquid was sonicated with a probe sonicator until a homogeneous dispersion with no visible sedimentation was obtained. The modified liquid was subsequently mixed with the acrylic resin powder at a powder-to-liquid weight ratio of 2:1. After a homogeneous paste was formed, the material was transferred into the molds. Following approximately 20 min of setting, the specimens were removed from the molds and finished using No. 80 and No. 1000 sandpapers. Adding AgNPs at 0.05% and 0.2% (w/w) did not visibly alter the handling characteristics of the self-cured acrylic resin; mixing, doughing, and setting proceeded similarly across groups, and all specimens were successfully fabricated using the same protocol. However, working time, doughing time, and peak exothermic temperature were not quantitatively measured. Because nanoparticle incorporation could theoretically influence polymerization kinetics, future studies should formally evaluate these parameters to confirm that AgNP-Root does not compromise clinical handling.

Characterization of Silver Nanoparticles

Dynamic Light Scattering

Dynamic light scattering (Zetasizer Nano ZS ZEN 3600, Malvern Instruments Ltd., UK) at a wavelength of 633 nm was used to measure the hydrodynamic particle size of the synthesized silver nanoparticles. Distilled water was used as the suspension medium. Particle size was determined based on the intensity distribution, while the polydispersity index was used to evaluate particle-size distribution. Measurements were performed according to ISO 22412(International Organization for Standardization. ISO 22412:2017. Particle size analysis — Dynamic light scattering (DLS). Geneva: ISO; 2017) at a concentration of 1 mg/mL.

Transmission Electron Microscopy

Transmission electron microscopy (TEM) was used to evaluate the size and morphology of the synthesized silver nanoparticles. TEM imaging was performed using a Philips EM 208S instrument operated at an accelerating voltage of 200 kV. Particle-size distribution was subsequently analyzed using ImageJ software.

Surface Finishing Protocol

For mechanical testing, specimens were finished with No. 80 and No. 1000 sandpapers to

achieve the dimensions specified by ISO 20795-1. For AFM analysis, specimens were prepared separately and wet-ground with 400, 1000, and 2000-grit silicon carbide papers for 60 seconds to produce a progressively polished surface suitable for topographic assessment. The finishing protocols therefore differed between the two test types: a coarser sequence was used for mechanical specimens to standardize dimensions, whereas a finer, progressively polished sequence was used for AFM specimens to minimize surface artifacts. All specimens were cleaned with air pressure before testing.

Mechanical Experiments

A three-point bending test was performed using a universal testing machine (ZWICK/ ROELL ZO20, Germany) to measure the flexural strength and flexural modulus of the acrylic resin nanocomposites according to ISO 20795-2(International Organization for Standardization. ISO 20795-2:2013. Dentistry — Base polymers — Part 2: Orthodontic base polymers. Geneva: ISO; 2013). Rectangular specimens were prepared using four-part brass molds. Following polymerization, the specimens were removed from the molds and immersed in distilled water at 37°C for 50 h, in accordance with ISO 20795-2:2013. The specimens were subsequently dried and finished using No. 80 and No. 1000 sandpapers as previously stated. The final specimen dimensions (64×10×3.3 mm) were measured using calipers and entered into the testing software.

Before mechanical testing, the specimens were immersed in distilled water. Testing was performed immediately after removing the specimens from water. Flexural strength was measured by a three-point bending test with a 500-N load cell at a crosshead speed of 5 mm/min and a span length of 50 mm until specimen fracture, in accordance with ISO 20795-2:2013. Nine specimens were tested for each composition (n=9 per group). Flexural modulus was calculated from the load and displacement data within the linear region of the load–displacement curve.

Surface Roughness

Atomic force microscopy (AFM) was used to evaluate the surface roughness of the acrylic resin nanocomposites. Measurements were performed using an AFM system (JPK NanoWizard II, Germany) in non-contact mode. To standardize the surface, all the samples were wet-ground with 400-, 1000-, and 2000-grit silicon carbide grinding papers for 60 seconds. Afterward, all the samples were cleaned with air pressure. The scanning area was 10×10 μm^2, with an image resolution of 256×256 pixels. Finally, the average values of surface roughness were determined for each group.

Antimicrobial Assays

Standard strains of *L. acidophilus* (ATCC 4356), *S. mutans* (ATCC 35668), and *C. albicans* (ATCC 14053) were obtained from the Iranian Biological Resource Center, Tehran, Iran. The microbial strains were cultured in brain heart infusion (BHI) broth (Merck, Germany) and incubated at 37°C for 24 h, according to each microorganism's growth requirements. *S. mutans* was cultured under anaerobic conditions in an anaerobic jar, whereas *L. acidophilus* and *C. albicans* were cultured under aerobic conditions. The logarithmic growth phase of each microorganism was adjusted to a 0.5 McFarland standard, corresponding to about 1.5×10^8 CFU/mL for bacteria but about $1–5\times10^6$ CFU/mL for Candida. This concentration was verified by measuring optical density at 600 nm (OD_{600} = 0.08–0.13) using a spectrophotometer. The antimicrobial effects of AgNP-TSC and AgNP-root on the tested microorganisms were evaluated using two different assays.

Eluted Component Test

The eluted component test was performed according to the method described by Arab et al. (24), with minor modifications. Briefly, acrylic resin discs were immersed in wells containing 1 mL of sterile saline. Acrylic resin discs (10 mm in diameter and 4 mm in thickness) were prepared using standardized brass molds. Three discs were prepared for each experimental group (n = 3). Following polymerization, the specimens were removed from the molds and sterilized by exposure to ultraviolet (UV) radiation for 2 h (25). For the eluted component test, the discs were immersed in 1 mL of sterile saline for 24 h. After 24 h of incubation, 50 µL of the elution medium was collected from each well and separately mixed with 50 µL of a microbial suspension containing 1.5×10^8 CFU/mL. The mixtures were incubated in a shaking incubator at 37°C and 300 rpm for 24 h. Subsequently, serial dilutions were prepared, and 10 µL of each appropriate dilution was spread onto BHI agar plates. Following incubation at 37°C for 24 h, viable microbial counts were determined and expressed as CFU/mL. Each experiment was performed in triplicate (24,25).

Biofilm Formation Test

The biofilm formation assay was performed based on the method described by Arab et al. (24), with modifications. Briefly, acrylic resin discs were

placed in tubes containing microbial suspensions of each tested microorganism at a concentration of 1.5×10^8 CFU/mL and incubated at 37°C for 48 h to allow biofilm formation on the disc surfaces. Following incubation, the discs were carefully removed using sterile forceps and gently washed with sterile saline to remove non-adherent planktonic microorganisms. Each disc was then transferred to a separate tube containing 1 mL of sterile saline. The attached biofilm was detached by sonication using a sonicator operating at 50 kHz and 150 W. The resulting suspensions were serially diluted as required, and 10 µL of the appropriate dilution was spread onto BHI agar plates. After incubation at 37°C for 24 h, viable bacterial counts were determined and expressed as CFU/mL. Each experimental group included three specimens (n = 3).

Statistical Analysis

Sample sizes were selected based on ISO 20795-1 recommendations for flexural testing (n=9 per group), standard AFM practice (n=5 per group), and standard microbiological triplicate protocols. A formal a priori power calculation was not performed because the study was exploratory in nature and no preliminary data were available to estimate effect sizes for the primary outcomes; sample sizes were therefore consistent with established standards and with previous in vitro studies of nanoparticle-modified acrylic resins (7,10).

All statistical analyses were performed using SPSS 27.0 (IBM, Armonk, NY, USA). The Kolmogorov–Smirnov test was used to assess the normality of the data. Continuous variables were expressed as means and standard deviations, whereas categorical variables were expressed as counts and percentages. For comparisons between the five study groups, one-way analysis of variance (ANOVA), followed by post hoc Tukey tests, was applied to normally distributed data. For nonparametric data, the independent-samples Kruskal–Wallis test was used for overall comparisons, and significance values were adjusted by the Bonferroni correction for multiple tests. A two-sided P-value<0.05 was considered statistically significant.

Results

Nanoparticle Characterization

DLS was used to characterize the hydrodynamic size distributions of the synthesized silver nanoparticles. For AgNP-TSC, the particle size distribution ranged from 30 to 245 nm, with mean hydrodynamic diameters of 158.15, 54.58, and 38.22 nm for the intensity-, volume-, and number-weighted distributions, respectively. The corresponding mean diameters for AgNP-root were 223.80, 95.67, and 60.71 nm, with a particle size range of 30–228 nm. AgNP-root exhibited a greater proportion of particles below 100 nm compared with AgNP-TSC (Figure 1).

TEM images showed predominantly spherical nanoparticles in both preparations. AgNP-TSC exhibited a broader apparent particle size distribution (5–60 nm), with a mean particle size of 16.5 nm, whereas AgNP-root showed a narrower distribution (15–42 nm), with a mean particle size of 32.3 nm. As shown in Figure 2, a greater apparent particle aggregation was observed in the AgNP-TSC preparation.

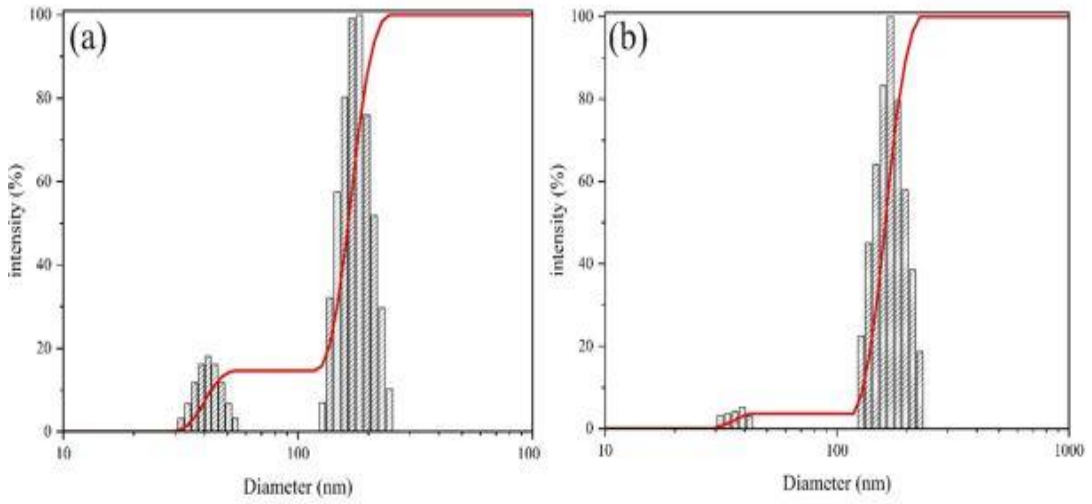


Figure 1. Particle size distributions of AgNP-TSC (a) and AgNP-Root (b) determined by dynamic light scattering.

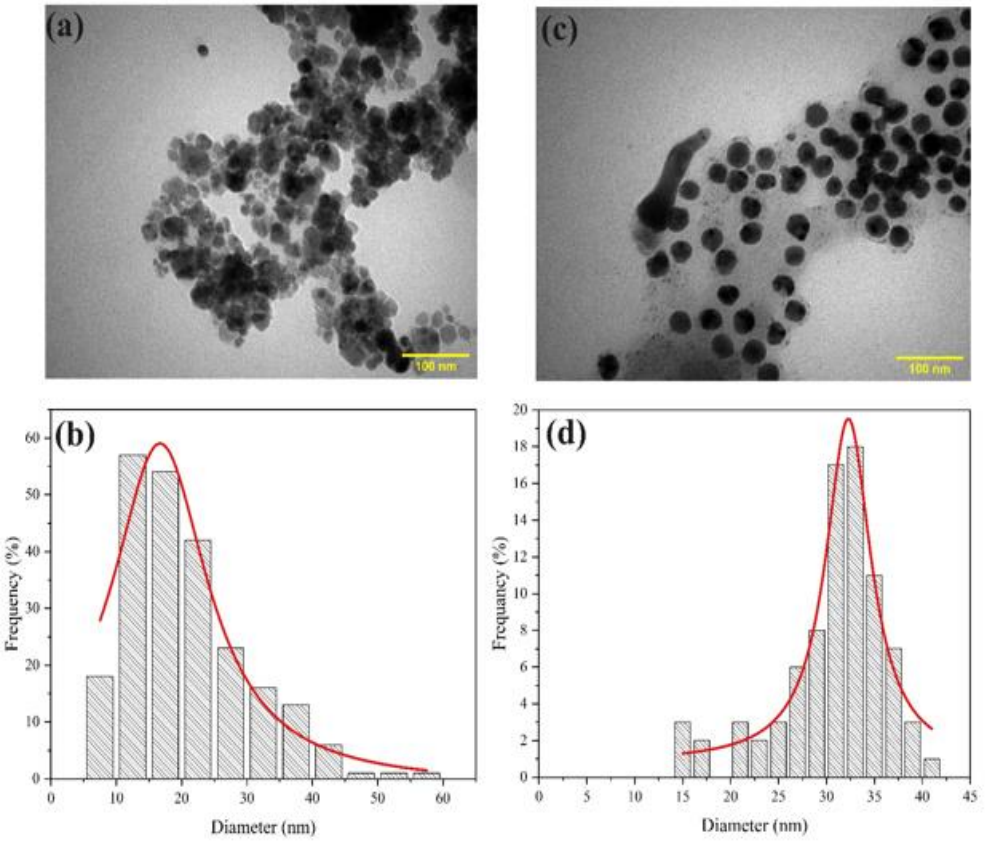


Figure 2. TEM characterization of the synthesized nanoparticles and corresponding size-distribution analyses. TEM image of AgNP-TSC (a) and its particle size distribution histogram (b); TEM image of AgNP-Root (c) and its particle size distribution histogram (d).

AFM was used to characterize the surface topography and roughness of the orthodontic acrylic resin nanocomposites containing either 0.05% or 0.2% AgNP-TSC or AgNP-root. Five specimens were evaluated for each group, and surface roughness measurements were compared between the study groups using one-way ANOVA, followed by post hoc Tukey tests. The surface

roughness values (Rq) were 78.5 ± 27.8, 150 ± 52.8, 64.5 ± 10.8, 149 ± 24.8, and 106.5 ± 51.91 nm for the control, 0.05% AgNP-TSC, 0.2% AgNP-TSC, 0.05% AgNP-root, and 0.2% AgNP-root groups, respectively. Data are presented as mean ± standard error (SE) (n = 5). One-way ANOVA revealed no statistically significant differences among the groups (P = 0.311) (Figure 3).

Flexural strength and flexural modulus were evaluated across the five groups, with nine specimens analyzed per group (Figure 4). The groups comprised the control, 0.05% AgNP-TSC, 0.2% AgNP-TSC, 0.05% AgNP-root, and 0.2% AgNP-root groups. Statistical comparisons were performed using one-way ANOVA, followed by post hoc Tukey tests. Mean flexural strength was 60.5±18 MPa in the control group, 57.8±10.5 MPa for 0.05% AgNP-TSC, 52.5±25.5 MPa for 0.2% AgNP-TSC, 55±36 MPa for 0.05% AgNP-root, and 56.5±41 MPa for 0.2% AgNP-root (P=0.95). The incorporation of AgNP-TSC or AgNP-root at both concentrations did not significantly affect the flexural strength of the acrylic resin (P>0.05). Mean flexural modulus was 2.35±0.15 GPa in the control group, 2.12±0.48 GPa for 0.05% AgNP-TSC, 1.9±1.05 GPa for 0.2% AgNP-TSC, 2.2±0.45 GPa for 0.05% AgNP-root, and 2.12±0.6 GPa for 0.2% AgNP-root; the 0.2% AgNP-TSC group differed significantly from the control group (P<0.0001), whereas the 0.05% AgNP-TSC, 0.05% AgNP-root, and 0.2% AgNP-root groups did not differ significantly from the control group (P>0.05).

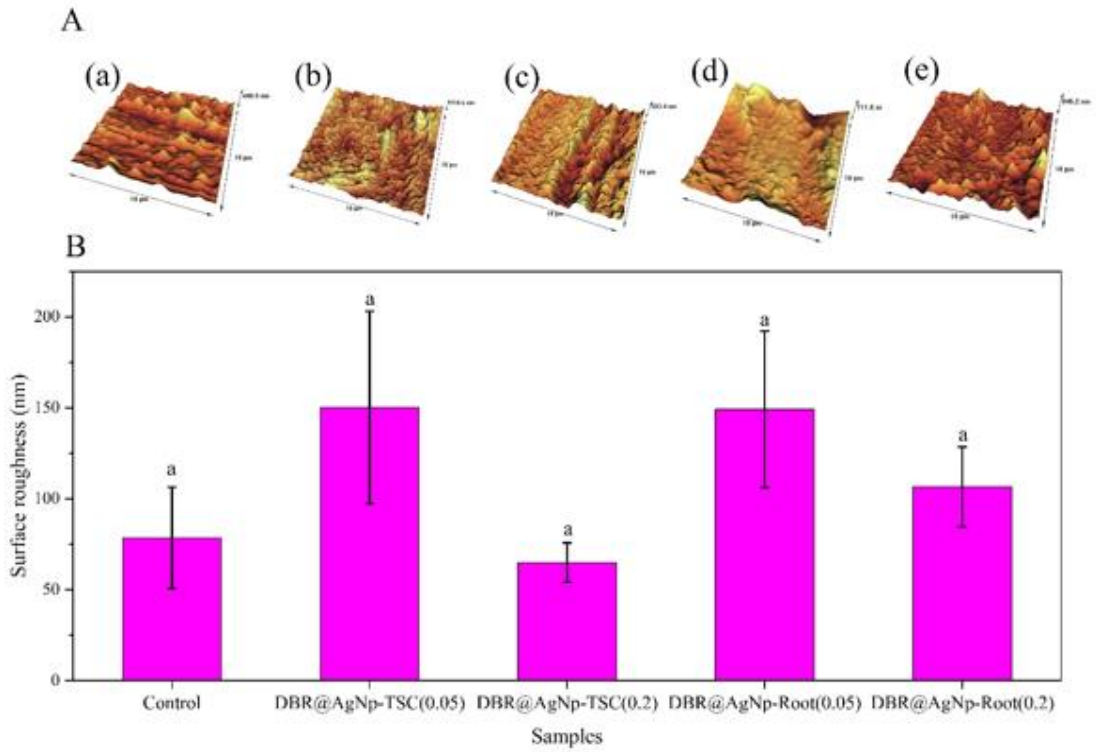


Figure 3. A) AFM images of the nanocomposites: (a) control, (b) 0.05% AgNP-TSC, (c) 0.2% AgNP-TSC, (d) 0.05% AgNP-Root, and (e) 0.2% AgNP-Root. (B) Surface roughness of the orthodontic acrylic resin nanocomposites across the five groups.

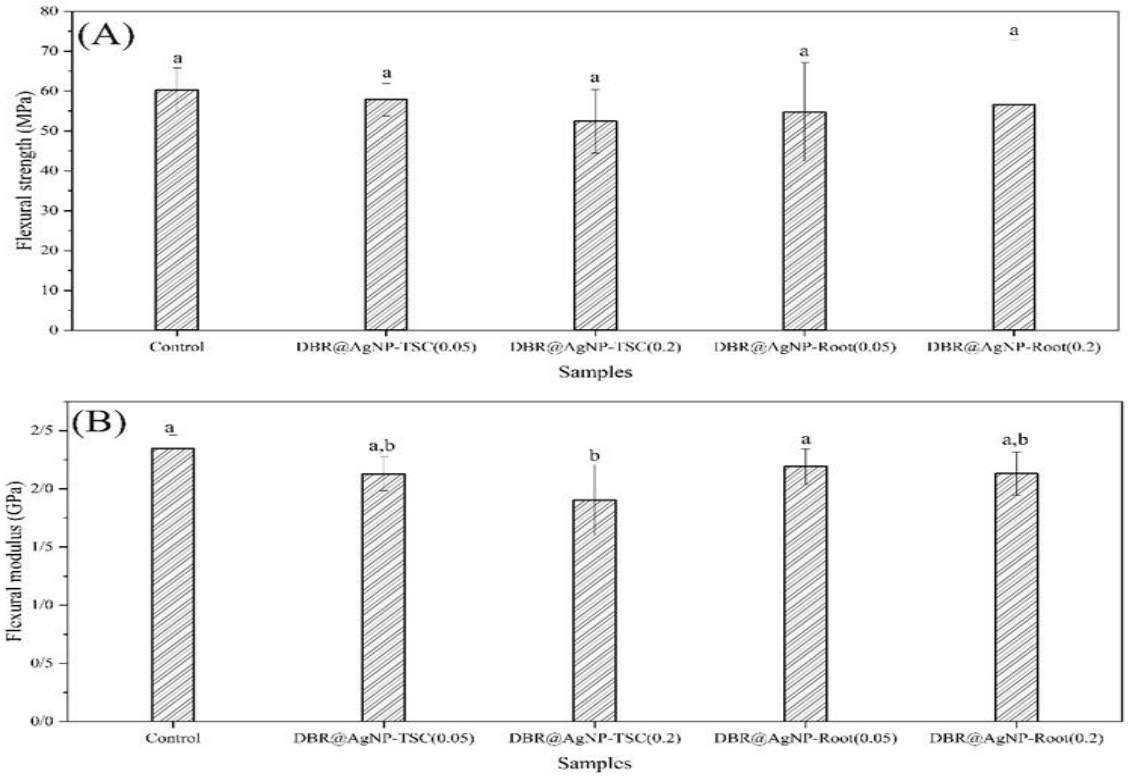


Figure 4. Flexural strength (A) and flexural modulus (B) of the orthodontic acrylic resin nanocomposites. Statistical significance was indicated by different superscript letters, whereas groups sharing the same letter were not significantly different.

Microbial Outcomes

The microbial counts of *L. acidophilus, S. mutans,* and *C. albicans* were evaluated using the ECT and biofilm formation assays. Comparisons were performed between the five study groups (0.05% AgNP-root, 0.2% AgNP-root, 0.05% AgNP-TSC, 0.2% AgNP-TSC, and the control). Overall differences between the five groups were assessed using the independent-samples Kruskal–Wallis test. When a significant overall difference was detected, pairwise comparisons were subsequently performed with Bonferroni adjustment.

L. acidophilus

Under the ECT condition, the control group exhibited the highest mean *L. acidophilus* count (3.8×10^5 CFU/mL). Compared with the control group, both the 0.05% and 0.2% AgNP-root groups exhibited significantly lower bacterial counts (1.3×10^5 CFU/mL for both concentrations; Bonferroni-adjusted P=0.035 and Bonferroni-adjusted P=0.047, respectively). In contrast, neither AgNP-TSC-treated group differed significantly from the control group (Bonferroni-adjusted P>0.05).

In the biofilm formation assay, the lowest mean *L. acidophilus* count was observed in the 0.05% AgNP-root group (3.8×10^3 CFU/mL), followed by the 0.2% AgNP-root group (1.0×10^4 CFU/mL). The mean counts in the 0.05% AgNP-TSC, 0.2% AgNP-TSC, and control groups were 3.4×10^5, 1.7×10^5, and 1.7×10^5 CFU/mL, respectively. No statistically significant differences were observed between the study groups (Bonferroni-adjusted P>0.05).

S. mutans

Under the ECT condition, the 0.2% AgNP-root group exhibited the lowest mean *S. mutans* count, with a statistically significant difference from the control group (2.1×10^3 CFU/mL vs. 2.7×10^4 CFU/mL, Bonferroni-adjusted P=0.045). Despite the apparent reduction in bacterial counts of other AgNP-treated groups, pairwise comparisons revealed no significant differences from the control group (Bonferroni-adjusted P>0.05).

In the biofilm formation assay, the mean *S. mutans* counts in the 0.05% AgNP-root, 0.2% AgNP-root, 0.05% AgNP-TSC, 0.2% AgNP-TSC, and control groups were 1.1×10^3, 1.1×10^3, 7.0×10^3, 8.0×10^3, and 7.6×10^3 CFU/mL, respectively. However, the differences were not significant (Bonferroni-adjusted P>0.05).

C. albicans

Under the ECT condition, the mean *C. albicans* counts were 7.0×10^6, 3.6×10^6, 1.9×10^6, 2.6×10^6,

and 4.6×10⁶ CFU/mL in the 0.05% AgNP-root, 0.2% AgNP-root, 0.05% AgNP-TSC, 0.2% AgNP-TSC, and control groups, respectively. A statistically significant difference was observed between the 0.05% AgNP-root and 0.05% AgNP-TSC groups (Bonferroni-adjusted P=0.025).

In the biofilm formation assay, the mean *C. albicans* biofilm counts were 4.8×10⁶, 1.6×10⁶, 1.9×10⁶, and 2.3×10⁶ CFU/mL in the 0.05% AgNP-root, 0.2% AgNP-root, 0.05% AgNP-TSC, and 0.2% AgNP-TSC groups, respectively, compared with 5.3×10⁶ CFU/mL in the control group. Although numerical differences in Candida counts were observed between the study groups, none of these differences reached statistical significance. Figure 5 presents the results of the ECT and biofilm formation assays for *L. acidophilus, S. mutans,* and *C. albicans*.

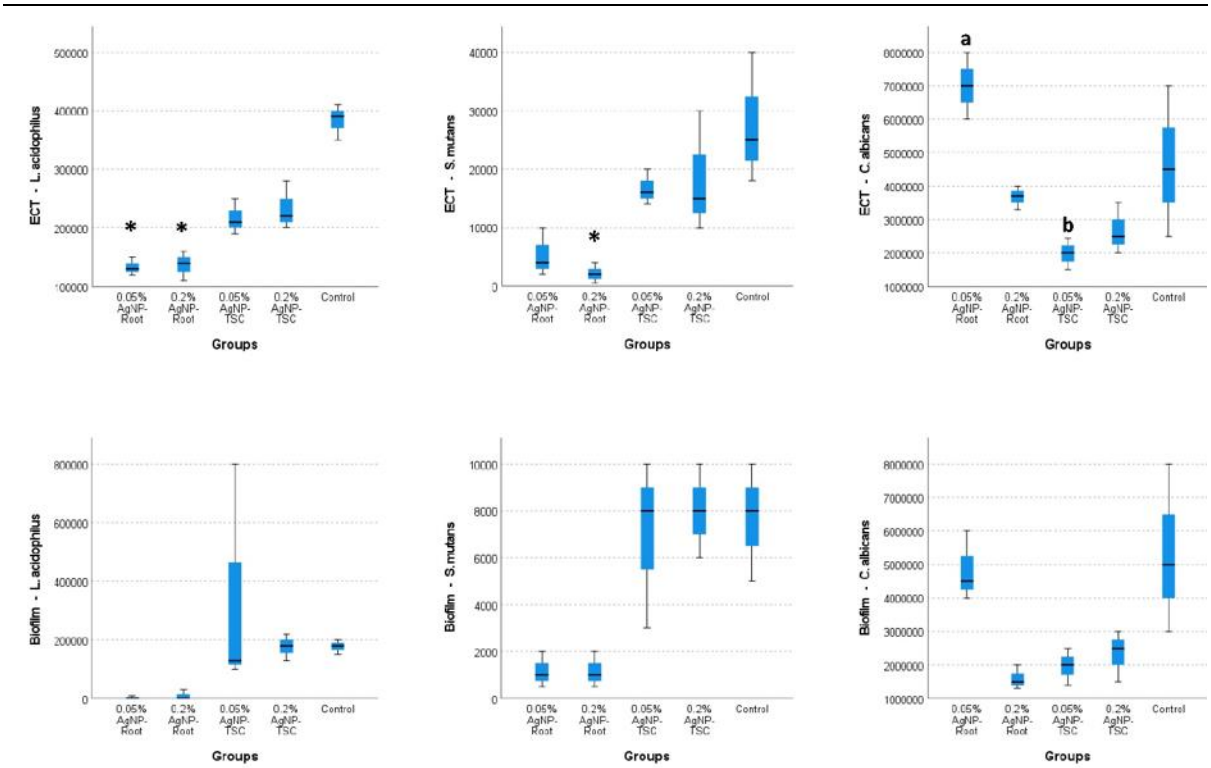


Figure 5. Microbial counts of L. acidophilus, S. mutans, and C. albicans following the eluted component test and biofilm formation assay. Asterisks indicate statistically significant differences compared with the control group. Different superscript letters indicate statistically significant differences between groups.

Discussion

This study evaluated the effects of chemically synthesized trisodium citrate-stabilized silver nanoparticles (AgNP-TSC) and R. palmatum-mediated silver nanoparticles (AgNP-root) on the mechanical, surface, and antimicrobial properties of orthodontic acrylic resin, while characterizing the particle size distributions and morphology of the two nanoparticle preparations. By directly comparing two synthesis strategies within a standardized experimental model, this study extends previous research that has primarily investigated the antimicrobial activity or mechanical effects of nanoparticle-modified acrylic resins separately. The findings indicate that nanoparticle formulation was associated with differences in selected physicochemical, mechanical, and antimicrobial outcomes. Although neither formulation significantly affected flexural strength or surface roughness, AgNP-root exhibited lower apparent aggregation and a narrower particle size distribution in TEM images. In contrast, AgNP-TSC was associated with greater aggregation and a significant reduction in flexural modulus at the highest concentration tested. AgNP-root also demonstrated a comparatively favorable antimicrobial response, particularly against *L. acidophilus* under the ECT condition. These findings suggest that nanoparticle characteristics may influence the functional performance of orthodontic acrylic resin nanocomposites, although

the mechanisms underlying the observed differences remain to be established. The two nanoparticle preparations differed in their physicochemical characteristics. TEM exhibited a smaller mean primary particle size for AgNP-TSC (16.5 nm) than for AgNP-root (32.3 nm). DLS showed a lower intensity-weighted mean diameter for AgNP-TSC (158.15 nm) than for AgNP-root (223.80 nm), although AgNP-root had a greater proportion of particles below 100 nm.

Considered alongside the narrower TEM size distribution and lower apparent aggregation observed qualitatively for AgNP-root, these results suggest differences in particle size distribution and aggregation behavior rather than a uniformly smaller particle size across all measurements. The apparent discrepancy between TEM and DLS measurements reflects the different principles underlying these techniques. TEM measures the metallic core diameter of dried nanoparticles, whereas DLS determines the hydrodynamic diameter in suspension, including the solvation layer and reflecting the presence of aggregates. The hydrodynamic-to-core diameter ratio was approximately 9.6 for AgNP-TSC (158.15 vs. 16.5 nm) and 6.9 for AgNP-root (223.80 vs. 32.3 nm), consistent with greater aggregation in the chemically synthesized preparation. Although zeta potential was not measured in the present study—a recognized limitation—the narrower TEM size distribution and lower apparent aggregation of AgNP-root are consistent with phytochemical-mediated steric and electrostatic stabilization by R. palmatum polyphenols, flavonoids, and anthraquinones, as reported previously (18,21,26-30). Direct measurement of zeta potential and surface chemistry would be required to confirm this proposed stabilization mechanism.

These physicochemical differences may affect the mechanical behavior of the resulting nanocomposites. In polymer-based materials, uniform filler dispersion can increase the effective interfacial area between the filler and matrix and potentially facilitate stress transfer. In contrast, aggregation may create structural heterogeneities and localized stress concentration sites (4,7). Previous investigations of acrylic resin systems have similarly highlighted the importance of nanoparticle dispersion. Shahabi et al. (7) associated deterioration in the flexural and compressive properties of acrylic resin containing chitosan nanoparticles with nanoparticle agglomeration, while Esmaeilzadeh et al. (4) emphasized the relevance of colloidal stability to nanoparticle distribution within an acrylic matrix. In the present study, neither AgNP-TSC nor AgNP-root significantly affected flexural strength. However, flexural modulus was significantly lower in the 0.2% AgNP-TSC group, whereas neither AgNP-root group differed significantly from the control. This selective reduction in modulus may relate to differences in aggregation behavior or interactions between the nanoparticles and the polymer matrix. Because nanoparticle dispersion within the polymerized resin was not directly assessed, this explanation remains hypothetical rather than a demonstrated mechanism.

The present mechanical findings are broadly consistent with previous research showing that the effects of nanoparticle incorporation depend on filler characteristics, concentration, and interactions with the polymer matrix. Köroğlu et al. (10) reported concentration-dependent effects of silver nanoparticles on the mechanical properties of acrylic resin, with lower concentrations generally associated with more favorable outcomes. Shahabi et al. (7) likewise attributed reductions in flexural and compressive properties to nanoparticle agglomeration and disruption of the acrylic matrix. Esmaeilzadeh et al. (4) demonstrated that improvements in antimicrobial activity may coincide with reductions in flexural properties, depending on nanoparticle characteristics and matrix interactions. Comparable variability has been reported for other nanofillers. Oyar et al. (20) observed improved flexural strength after incorporating low concentrations of gold nanoparticles, whereas studies involving TiO_2, SiO_2, nanodiamond, and chitosan nanoparticles reported different mechanical responses depending on filler characteristics and matrix interactions (4,7). Collectively, these findings indicate that nanoparticle concentration alone does not determine material performance; filler physicochemical properties and dispersion must also be considered. The absence of statistically significant differences in flexural strength and modulus between the AgNP-root groups and the control is therefore noteworthy. Although this finding is consistent with mechanical compatibility under the conditions investigated, it does not establish equivalence or demonstrate that the nanoparticles were uniformly distributed throughout the polymer matrix, because the distribution of nanoparticles within the polymerized resin was not directly characterized.

Surface roughness was not significantly affected by either nanoparticle formulation at the concentrations tested. This finding suggests that nanoparticle incorporation did not produce detectable changes in surface topography under the present experimental conditions. Because

surface roughness can influence microbial adhesion and subsequent biofilm development, its preservation is relevant when evaluating antimicrobial modifications of orthodontic acrylic resin. The absence of significant differences in roughness also indicates that the observed antimicrobial responses were not accompanied by statistically detectable changes in this surface parameter. This interpretation aligns with Jasso-Ruiz et al. (11), who reported reduced bacterial adhesion after silver nanoparticle modification of dental materials despite limited changes in surface characteristics. Similarly, Esmaeilzadeh et al. (4) observed antibacterial activity in nanoparticle-modified orthodontic acrylic resin alongside relatively modest changes in roughness. However, findings in this area are not entirely consistent. De Matteis et al. (31), for example, reported a significant reduction in surface roughness after incorporating silver nanoparticles into polymethylmethacrylate (PMMA)-based denture materials. Differences in nanoparticle composition, synthesis methods, concentrations, dispersion, and specimen-processing conditions may contribute to these variations. Overall, the present findings suggest that substantial changes in surface topography were not necessary for the antimicrobial responses observed in the nanoparticle-containing groups.

The microbiological findings further indicate that antimicrobial activity depended on both nanoparticle formulation and the microorganism tested. Under the ECT condition, *L. acidophilus* showed the clearest response, with AgNP-root producing statistically significant reductions. Although lower viable counts were also observed for *S. mutans*, the difference reached statistical significance only in the 0.2% AgNP-root group. For *C. albicans*, AgNP-TSC yielded lower mean counts than AgNP-root at both concentrations; however, a statistically significant difference was detected only between the 0.05% AgNP-root and 0.05% AgNP-TSC groups. These findings demonstrate that the antimicrobial response was not uniform across the tested microorganisms or assay conditions. Such variability is biologically plausible because microorganisms differ in cell envelope structure, membrane composition, metabolic activity, and susceptibility to antimicrobial stress. Nevertheless, this study did not directly investigate the biological mechanisms underlying these microorganism-dependent responses.

The comparatively favorable response of AgNP-root against *L. acidophilus* may be related to its physicochemical characteristics, although this interpretation requires caution. Lower apparent aggregation could potentially influence nanoparticle availability and interactions with the surrounding environment. In addition, phytochemicals associated with the nanoparticle surface may contribute to colloidal stabilization and potentially influence biological activity. Arokiyaraj et al. (21) reported favorable physicochemical characteristics and antimicrobial activity for silver nanoparticles synthesized using R. palmatum. In contrast, Bahraminezhad et al. (18) observed greater antibacterial activity for green-synthesized silver nanoparticles than for chemically synthesized counterparts and discussed the possible contribution of colloidal stability and phytochemical-mediated surface stabilization. These findings are broadly consistent with the present observations; however, the cited studies evaluated nanoparticle preparations rather than nanoparticle-modified orthodontic acrylic resin and therefore do not establish the same mechanisms in the present material system. The response of *S. mutans* is also compatible with the findings of Jasso-Ruiz et al. (11), who reported reduced adhesion of cariogenic streptococci following silver nanoparticle modification of dental materials. Similarly, the numerical differences observed for *C. albicans* should be interpreted in light of the limited statistical evidence. Esmaeilzadeh et al. (4) and Pourhajibagher et al. (6, 14) have also shown that antimicrobial efficacy can vary with nanoparticle characteristics, concentration, and microorganism-specific susceptibility. Collectively, these findings underscore the importance of evaluating multiple microorganisms and distinguishing between assay-specific responses when assessing antimicrobial dental materials.

The potential contribution of plant-derived compounds and silver ion release warrants further investigation. Although phytochemicals associated with AgNP-root may have contributed to its stabilization or biological response, the present study did not directly assess their presence, composition, or independent antimicrobial effects. Likewise, silver ion release was not quantified, preventing determination of the relative contributions of nanoparticle-associated effects and ion-mediated antimicrobial activity. Furthermore, nanoparticle distribution within the polymerized resin was not examined directly. Consequently, neither improved nanoparticle availability nor phytochemical-mediated antimicrobial activity can be established as the mechanism underlying the observed differences. These explanations should therefore be regarded as plausible hypotheses requiring targeted experimental verification.

Because biofilm formation is particularly relevant to microbial colonization of dental materials, the present study also assessed biofilm-associated viable counts. AgNP-root showed numerically lower biofilm counts for *L. acidophilus*, *S. mutans*, and *C. albicans*. However, these trends should be interpreted cautiously because they were not accompanied by consistent, statistically significant differences across biofilm outcomes. The findings therefore provide limited evidence of an effect on biofilm formation and should not be interpreted as demonstrating broad-spectrum antibiofilm efficacy. Nevertheless, the observed trends are compatible with previous reports of favorable antibacterial activity associated with green-synthesized silver nanoparticles (18), and support further investigation using larger sample sizes and more clinically representative biofilm models. The divergence between the ECT and biofilm assays merits consideration. In the ECT, antimicrobial activity depends on silver ions and nanoparticle-associated components released into the surrounding medium, which can readily interact with planktonic cells. In the biofilm assay, by contrast, microorganisms are embedded within an extracellular polymeric substance (EPS) matrix that can limit antimicrobial agent diffusion and shield embedded cells from environmental stress. The observation that significant effects were detected under ECT conditions but not in intact biofilms is therefore biologically plausible and suggests that, at the concentrations tested, silver ion release was sufficient to inhibit planktonic growth but insufficient to penetrate and disrupt established EPS matrices within the 48-hour biofilm model. This interpretation is consistent with the recognized role of EPS as a diffusion barrier and with the short duration of the biofilm assay, which may not have permitted the accumulation of a sufficient inhibitory dose at the biofilm–substrate interface. It should be emphasized, however, that silver ion release was not quantified in the present study; consequently, this mechanistic explanation remains hypothetical and requires confirmation through silver release kinetics and EPS penetration studies.

From a materials perspective, simultaneously assessing physicochemical, mechanical, surface, and microbiological outcomes is important because an antimicrobial modification must preserve the functional integrity of orthodontic acrylic resin nanocomposites. Under the conditions investigated, AgNP-root did not show statistically significant changes in flexural strength, flexural modulus, or surface roughness relative to the control, while showing a favorable antibacterial response against *L. acidophilus* and S. mutans under the ECT condition. These findings identify AgNP-root as a potentially promising formulation for further evaluation. Nevertheless, the observed antibacterial responses did not demonstrate clinical effectiveness. In addition, although both formulations were evaluated using the same resin, concentrations, specimen-fabrication procedures, and analytical protocols, the synthesis routes may have altered multiple nanoparticle characteristics simultaneously. However, the specific mechanisms underlying these differences were not fully characterized. Based on the present results alone, the effects of synthesis strategy cannot be separated from other formulation-specific properties.

An important consideration for the clinical translation of AgNP-modified orthodontic acrylic resins is aesthetic appearance. Incorporation of silver nanoparticles into PMMA has been associated with concentration-dependent brownish, yellowish, or greyish discoloration, which is particularly relevant because removable orthodontic appliances are frequently visible during wear. Although a formal spectrophotometric color assessment (ΔE) was not performed in the present study, no overt discoloration was noted during specimen preparation and handling in either the 0.05% or 0.2% groups; however, this observation was qualitative and cannot substitute for instrumental color measurement. Because even visually subtle changes may be unacceptable to patients, future studies should incorporate quantitative color stability analysis, including ΔE evaluation before and after aging, to establish the aesthetic acceptability of AgNP-root–modified resins at clinically relevant concentrations.

Several limitations should be acknowledged. First, the study was conducted entirely under controlled in vitro conditions and therefore does not reproduce the complexity of the oral environment, where salivary components, pH fluctuations, enzymatic activity, mechanical loading, host responses, and multispecies microbial interactions may affect material performance. Second, the long-term stability of the modified orthodontic acrylic resin was not evaluated; consequently, the effects of aging on nanoparticle dispersion, silver ion release, mechanical integrity, and sustained antimicrobial activity remain unknown. Third, biological safety was not assessed. Cytotoxicity, genotoxicity, oxidative stress, inflammatory responses, and long-term biocompatibility must be investigated before clinical translation can be considered. Fourth, although TEM, DLS, and AFM provided useful

information on nanoparticle morphology, hydrodynamic size, and surface characteristics, further characterization using techniques such as X-ray diffraction, Fourier-transform infrared spectroscopy, zeta-potential analysis, and elemental analysis would help clarify nanoparticle composition, surface chemistry, colloidal stability, and interactions with the polymer matrix. The variability of plant-derived compounds associated with the source material and extraction conditions also highlights the need to standardize the green synthesis process. Future studies should therefore evaluate the durability and biological safety of AgNP-root under clinically relevant conditions. Long-term performance, dynamic oral environment simulation, multispecies biofilm models, quantitative silver ion release measurements, and direct mapping of nanoparticle distribution within the polymer matrix would help clarify the mechanisms underlying the observed mechanical and antimicrobial responses. Finally, standardization of R. palmatum-mediated synthesis will be essential to determine whether its physicochemical characteristics and material performance can be reproduced across different extract batches and synthesis conditions.

Conclusion

Under the conditions investigated, the synthesis strategy of silver nanoparticles was associated with differences in the physicochemical and functional characteristics of nanoparticle-modified orthodontic acrylic resin. AgNP-root exhibited lower apparent aggregation and a narrower TEM particle size distribution than AgNP-TSC. At the same time, neither AgNP-root concentration produced statistically significant differences in flexural strength, flexural modulus, or surface roughness relative to the control. Antimicrobial responses varied by microorganism and assay, with the clearest statistically significant antibacterial effect against *L. acidophilus* under the ECT condition. These findings suggest that nanoparticle physicochemical characteristics may be relevant to developing antimicrobial orthodontic acrylic resin materials. However, the absence of direct measurements of nanoparticle distribution within the polymer matrix, silver ion release, and biological safety limits mechanistic interpretation and precludes conclusions regarding clinical effectiveness.

Acknowledgment

The authors would like to thank Dr. Mohammad Atai and the Iran Polymer and Petrochemical Institute (IPPI) for their cooperation and technical support during the nanoparticle preparation and characterization procedures.

The authors gratefully acknowledge the Statistical Analysis Center of Shiraz University of Medical Sciences for its valuable statistical consultation.

Conflicts of Interest

The authors declare no conflicts of interest.

Funding

This research did not receive any specific grant from Funding agencies in the public, commercial, or not-for-profit sector

Data Availability

The data supporting the findings of this study are available from the corresponding author upon reasonable request.

Author Contributions

Ali Ghaboos: Conceptualization, Methodology, Investigation, Data Curation, Formal Analysis, Writing – Original Draft.

Farzaneh Golfeshan: Conceptualization, Methodology, Supervision, Validation, Writing – Review & Editing, Project Administration.

Mohammad Motamedifar: Methodology, Investigation, Validation, Writing – Review & Editing.

All authors contributed to the manuscript's development, critically reviewed it for important intellectual content, and approved the final version for publication.

All authors agree to be accountable for all aspects of the work and ensure that questions related to the accuracy or integrity of any part of the work are appropriately investigated and resolved.

References

1. Fu D, Shu X, Yao L, Zhou G, Ji M, Liao G, Zhu Y, Zou L. Unveiling the dual nature of Lactobacillus: from cariogenic threat to probiotic protector-a critical review with bibliometric analysis. Front Oral Health. 2025;6:1535233. doi: 10.3389/froh.2025.1535233.
2. Lucchese A, Bonini C, Noviello M, Lupo Stanghellini MT, Greco R, Peccatori J, et al. The effect of

removable orthodontic appliances on oral microbiota: a systematic review. Appl Sci. 2021;11(6):1-11. doi:10.3390/app11062881.
3. Rodríguez-Rentería M, Márquez-Preciado R, Ortiz-Magdaleno M, Bermeo-Escalona J, Sánchez-Vargas LO. Frequency of pathogenic microorganisms in removable orthodontic appliances and oral mucosa in children. J Clin Pediatr Dent. 2021;45(2):135-139. doi: 10.17796/1053-4625-45.2.11.
4. Esmaeilzadeh M, Divband B, Ranjkesh B, Pournaghi Azar F, Yeganeh Sefidan F, Kachoei M, Karimzadeh B. Antimicrobial and mechanical properties of orthodontic acrylic resin containing zinc oxide and titanium dioxide nanoparticles supported on 4A zeolite. Int J Dent. 2022;2022:8155971. doi: 10.1155/2022/8155971.
5. Alqutaibi AY, Baik A, Almuzaini SA, Farghal AE, Alnazzawi AA, Borzangy S, Aboalrejal AN, AbdElaziz MH, Mahmoud II, Zafar MS. Polymeric denture base materials: A Review. Polymers (Basel). 2023;15(15):1-27. doi: 10.3390/polym15153258.
6. Pourhajibagher M, Noroozian M, Ahmad Akhoundi MS, Bahador A. Antimicrobial effects and mechanical properties of poly(methyl methacrylate) as an orthodontic acrylic resin containing Curcumin-Nisin-poly(L-lactic acid) nanoparticle: an in vitro study. BMC Oral Health. 2022;22(1):1-10. doi: 10.1186/s12903-022-02197-z.
7. Shahabi M, Movahedi Fazel S, Rangrazi A. Incorporation of chitosan nanoparticles into a cold-cure orthodontic acrylic resin: effects on mechanical properties. Biomimetics (Basel). 2021;6(1):1-9. doi: 10.3390/biomimetics6010007.
8. Jandt KD, Watts DC. Nanotechnology in dentistry: Present and future perspectives on dental nanomaterials. Dent Mater. 2020;36(11):1365-1378. doi: 10.1016/j.dental.2020.08.006.
9. Umapathy VR, Natarajan PM, SumathiJones C, Swamikannu B, Johnson WM, Alagarsamy V, et al. Current trends and future perspectives on dental nanomaterials: an overview of nanotechnology strategies in dentistry. J King Saud Univ Sci. 2022;34(7):1-11. doi:10.1016/j.jksus.2022.102231.
10. Köroğlu A, Şahin O, Kürkçüoğlu I, Dede DÖ, Özdemir T, Hazer B. Silver nanoparticle incorporation effect on mechanical and thermal properties of denture base acrylic resins. J Appl Oral Sci. 2016;24(6):590-596. doi: 10.1590/1678-775720160185.
11. Jasso-Ruiz I, Velazquez-Enriquez U, Scougall-Vilchis RJ, Morales-Luckie RA, Sawada T, Yamaguchi R. Silver nanoparticles in orthodontics, a new alternative in bacterial inhibition: in vitro study. Prog Orthod. 2020;21(1):1-8. doi: 10.1186/s40510-020-00324-6.
12. Yin IX, Zhang J, Zhao IS, Mei ML, Li Q, Chu CH. The Antibacterial mechanism of silver nanoparticles and its application in dentistry. Int J Nanomedicine. 2020;15:2555-2562. doi: 10.2147/IJN.S246764.
13. Yudaev P, Chuev V, Klyukin B, Kuskov A, Mezhuev Y, Chistyakov E. Polymeric dental nanomaterials: Antimicrobial action. Polymers (Basel). 2022;14(5):1-24. doi: 10.3390/polym14050864.
14. Pourhajibagher M, Bahador A. Effects of incorporation of nanoparticles into dental acrylic resins on antimicrobial and physico-mechanical properties: A meta-analysis of in vitro studies. J Oral Biol Craniofac Res. 2022;12(5):557-568. doi: 10.1016/j.jobcr.2022.07.010.
15. Ying S, Guan Z, Ofoegbu PC, Clubb P, Rico C, He F, et al. Green synthesis of nanoparticles: current developments and limitations. Environ Technol Innov. 2022;26:102336. doi:10.1016/j.eti.2022.102336.
16. Jadoun S, Arif R, Jangid NK, Meena RK. Green synthesis of nanoparticles using plant extracts: a review. Environ Chem Lett. 2021;19(1):355-74. doi:10.1007/s10311-020-01074-x.
17. Rajeshkumar S, Bharath LV. Mechanism of plant-mediated synthesis of silver nanoparticles - A review on biomolecules involved, characterisation and antibacterial activity. Chem Biol Interact. 2017;273:219-227. doi: 10.1016/j.cbi.2017.06.019.
18. Bahraminezhad S, Mehrasbi MR, Homauoni P, Farahmandkia Z. A comparative analysis of the antibacterial effects of green-synthesized silver nanoparticles with chemically synthesized silver nanoparticles. J Hum Environ Health Promot. 2025;11(3):175-81. doi:10.61186/jhehp.11.3.175.
19. Gour A, Jain NK. Advances in green synthesis of nanoparticles. Artif Cells Nanomed Biotechnol. 2019;47(1):844-851. doi: 10.1080/21691401.2019.1577878.
20. Oyar P, Sana FA, Nasseri B, Durkan R. Effect of green gold nanoparticles synthesized with plant on the flexural strength of heat-polymerized acrylic resin. Niger J Clin Pract. 2018;21(10):1291-1295. doi: 10.4103/njcp.njcp_388_17.
21. Arokiyaraj S, Vincent S, Saravanan M, Lee Y, Oh YK, Kim KH. Green synthesis of silver nanoparticles using *Rheum palmatum* root extract and their antibacterial activity against Staphylococcus aureus and Pseudomonas aeruginosa. Artif Cells Nanomed Biotechnol. 2017;45(2):372-379. doi: 10.3109/21691401.2016.1160403.
22. Wani IA, Ganguly A, Ahmed J, Ahmad T. Silver nanoparticles: ultrasonic wave assisted synthesis, optical characterization and surface area studies. Mater Lett. 2011;65(3):520-2. doi:10.1016/j.matlet.2010.11.003.
23. Özarslan M, Bilgili Can D, Avcioglu NH, Çalışkan S. Effect of different polishing techniques on surface properties and bacterial adhesion on resin-ceramic CAD/CAM materials. Clin Oral Investig. 2022;26(8):5289-99.
24. Arab S, Bahador A, Sodagar A, Pourhajibagher M, Akhavan A, Hafith AN, et al. Antimicrobial properties of acrylic resin incorporated with propolis nanoparticles. Front Dent. 2021;18:29.
25. Gong SQ, Epasinghe DJ, Zhou B, Niu LN, Kimmerling KA, Rueggeberg FA, et al. Effect of water-aging on the antimicrobial activities of an ORMOSIL-containing orthodontic acrylic resin. Acta Biomater. 2013;9(6):6964-73.

26. Elia P, Zach R, Hazan S, Kolusheva S, Porat Z, Zeiri Y. Green synthesis of gold nanoparticles using plant extracts as reducing agents. Int J Nanomedicine. 2014;9:4007-21. doi: 10.2147/IJN.S57343.
27. Martínez-Castañón GA, Niño-Martínez N, Martínez-Gutierrez F, Martínez-Mendoza JR, Ruiz F. Synthesis and antibacterial activity of silver nanoparticles with different sizes. J Nanopart Res. 2008;10(8):1343-8. doi:10.1007/s11051-008-9428-6.
28. Jha AK, Prasad K, Prasad K, Kulkarni AR. Plant system: nature's nanofactory. Colloids Surf B Biointerfaces. 2009;73(2):219-23. doi: 10.1016/j.colsurfb.2009.05.018.
29. Arya V. Living systems: eco-friendly nanofactories. Dig J Nanomater Biostruct. 2010;5(1):9-21.
30. Gong X, Jadhav ND, Lonikar VV, Kulkarni AN, Zhang H, Sankapal BR, Ren J, Xu BB, Pathan HM, Ma Y, Lin Z, Witherspoon E, Wang Z, Guo Z. An overview of green synthesized silver nanoparticles towards bioactive antibacterial, antimicrobial and antifungal applications. Adv Colloid Interface Sci. 2024;323:103053. doi: 10.1016/j.cis.2023.103053.
31. De Matteis V, Cascione M, Toma CC, Albanese G, De Giorgi ML, Corsalini M, Rinaldi R. Silver nanoparticles addition in poly (Methyl Methacrylate) dental matrix: Topographic and antimycotic studies. Int J Mol Sci. 2019;20(19):1-14. doi: 10.3390/ijms20194691.